Kinetics of the Desorption of Surfactants and Proteins from Adsorption Layers at the Solution/Air Interface

V. B. Fainerman,[†] M. E. Leser,[‡] M. Michel,[‡] E. H. Lucassen-Reynders,[§] and R. Miller*,[⊥]

Medical Physicochemical Centre, Donetsk Medical University, 16 Ilych Avenue, 83003 Donetsk, Ukraine, Nestec Ltd., Nestlé Research Centre, Vers-chez-les-Blanc, CH-1000 Lausanne 26, Switzerland, Mathenesselaan 11, 2343 HA Oegstgeest, The Netherlands, and Max-Planck-Institut für Kolloid- und Grenzflächenforschung, Am Mühlenberg 1, 14424 Potsdam, Germany

Received: January 12, 2005; In Final Form: March 17, 2005

It is shown by experiments that the DeSNa desorption kinetics is governed by a pure diffusion mechanism, while the desorption of more surface active surfactants such as C_{13}DMPO and Triton X-100 obeys a mixed mechanism. The BLG desorption kinetics, as shown by experiments, is determined by a barrier mechanism. From the analysis of the temperature dependence of the BLG desorption kinetics it is possible to calculate the activation energy of this process, which is quite close to the free energy of BLG adsorption. The theoretical model of desorption kinetics predicts that these two energetic parameters are approximately equal to each other if the adsorption activation energy is low. This can explain the fact that the higher the adsorption activity of a substance is, the lower is its desorption rate.

Introduction

Replacing the bulk solution by the pure solvent, proteins desorb from solid surfaces very slowly.[1−3] The reason for this slow process is probably the remarkably high free Gibbs energy of adsorption of proteins. According to Norde and Haynes[1] the free energy of adsorption for proteins of a molecular mass of 100 kDa amounts to values between −125 and −500 kJ/mol. These results lead to the assumption that the adsorption kinetics of high-molecular mass proteins or colloidal particles at solid surfaces is an irreversible process (in analogy to the kinetically irreversible or unidirectional chemical reactions), neglecting the reverse flux of material from the surface into the bulk.[2,4]

In the same way we can see the adsorption of proteins at liquid interfaces. To our knowledge, the first quantitative analysis of the kinetics of protein desorption from spread monolayers was presented in ref 5. It was shown that the factors increasing the desorption rate are increased surface pressure, increase in protein bulk concentration, and agitation in the bulk phase. A detailed review of studies on protein desorption kinetics was presented by MacRitchie,[6] where the problem of reversibility and irreversibility of protein adsorption at liquid interfaces was discussed in much detail. It was shown, in particular, that (i) at low surface pressure (below 15 mN/m) there is virtually no desorption of proteins from spread monolayers into the pure solvent within a time scale of 2 h, (ii) the desorption rate is rather slow (and obeys a nondiffusional mechanism) at higher surface pressure, and (iii) the higher the protein molecular mass is, the higher is the surface pressure at which the desorption rate becomes measurable. In conclusion, MacRitchie indicated explicitly that the problem of reversibility of protein adsorption remains uncertain and should be the subject of future studies.[6]

Recent publications in this area have dealt with the kinetics of desorption from adsorbed protein layers. Svitova et al. proposed a convection cell in which the liquid in a cuvette is exchanged at a known flow rate.[7] The bubble formed in the filled cuvette remains during this exchange and provides information on the subsequent desorption process. The experiments were performed with a 0.01% BSA solution and showed no protein desorption during tens of hours, leading to the conclusion that BSA adsorbs irreversibly. Another option was proposed by Wege et al.,[8] who used a special coaxial double capillary. This equipment allows the exchange of the volume of a drop, i.e., to replace the protein solution in the drop completely by the pure buffer solution. A similar device was employed in ref 9, where the measuring cell was equipped with a special double dosing and coaxial double capillary system suitable to exchange the bulk solution in a drop by the pure solvent without disturbing the continuous analysis of its shape. It was shown that there is almost no desorption of β-casein, while for the β-lactoglobulin the desorption is very slow. An attempt was also made in ref 9 to analyze theoretically the nature of slow desorption of proteins and some surfactants from the viewpoint of desorption kinetics governed by a barrier mechanism. It was shown that the desorption activation energy is approximately equal to the adsorption free energy, which agrees qualitatively with many experimental results.

In this paper we present experimental results of desorption kinetics studies for surfactants of various nature and β−lactoglobulin (BLG) from adsorption layers. The temperature dependence of BLG desorption kinetics was determined in order to get access to the activation energy of the desorption process, so that a comparison with predictions of a recently proposed model[9] was possible.

Experimental Section

The experiments were performed by a bubble profile analysis tensiometer (PAT1, SINTERFACE),[10] similar to that used in ref 7. The measuring cell (volume $V = 20$ mL) had two pipes

* Corresponding author.
[†] Donetsk Medical University.
[‡] Nestec Ltd.
[§] Mathenesselaan 11.
[⊥] Max-Planck-Institut für Kolloid- und Grenzflächenforschung.

10.1021/jp050212o CCC: $30.25
Published on Web 04/14/2005

to supply the washing liquid into the lower part of the cell and to eject the solution from the upper part (from the surface of the liquid in the cell). As the flow of the washing liquid was constant ($L = 0.2$ mL/s), the liquid exchange time in the cell was $\tau = V/L = 100$ s. In this study an emerging bubble was employed that was formed at a steel capillary of 3 mm in diameter. We believe that for an elongated bubble the mixing in the measuring cell is almost ideal, because this configuration eliminates the thin liquid layer that may exist between a pendant bubble and a Teflon capillary.[7] To prevent the surfactant solution rising into the capillary, the capillary was filled by the solvent prior to the experimental run. For the experiments with proteins, the bubble was formed in the solvent (buffer solution). In these experiments, the bubble was first formed and then several surface tension measurements of the solvent (i.e., after a time period of ca. 20 s) were performed, before the solvent was replaced by the solution under study. To achieve such replacement, at least 10 cycles of complete replacement of the liquid in the cell were made. Assuming ideal mixing, as was shown in ref 7, after 10 cycles of replacement the concentration of the solution in the cell differs from the concentration of the washing solution by less than 0.01% ($\exp(-10)$). Finally, after the adsorption equilibrium was achieved, the solution was gradually replaced by the solvent. The procedure was continuous and replaced the solution in the cell by the solvent during 50 and more cycles.

The sample of β-lactoglobulin (BLG) from bovine milk was purchased from Sigma Chemical. The protein was used without further purification. The protein solutions were prepared in the presence of phosphate buffer (0.01 M of Na_2HPO_4 and NaH_2PO_4, pH 7.0).

The substances studied were the anionic surfactant sodium decyl sulfate (DeSNa) and nonionic surfactants Triton X-100 and tridecyl dimethyl phosphine oxide (C_{13}DMPO). DeSNa and C_{13}DMPO were synthesized and purified as described earlier.[11,12] Triton X-100 (from Aldrich) was used without any purification. The surface tension isotherms for these surfactants at 25 °C were presented in ref 13.

Theoretical Analysis of Desorption Rates. Assuming a combined mechanism for the adsorption and/or desorption kinetics involving the diffusion and adsorption/desorption barrier of any nature, the resulting rate of the whole process can be determined from the rates of diffusion and the barrier mechanisms:[14]

$$(\mathrm{d}\Gamma/\mathrm{d}t)^{-1} = (\mathrm{d}\Gamma/\mathrm{d}t)_{\mathrm{D}}^{-1} + (\mathrm{d}\Gamma/\mathrm{d}t)_{\mathrm{A}}^{-1} \quad (1)$$

where Γ is the adsorption, t is the time, the subscripts D and A refer to the diffusion and adsorption barrier mechanisms, respectively. It follows from eq 1 that the process rate is determined by its slowest stage, and if, for example, $(\mathrm{d}\Gamma/\mathrm{d}t)_{\mathrm{D}} \ll (\mathrm{d}\Gamma/\mathrm{d}t)_{\mathrm{A}}$, then the whole process can be regarded as diffusion controlled.

For a bubble in a cell with ideal mixing of the solution, the value of $(\mathrm{d}\Gamma/\mathrm{d}t)_{\mathrm{D}}$ can be easily calculated. Assume the dependencies of equilibrium surface tension of the solution γ and adsorption Γ on the bulk concentration c_{b} are known. At $t = 0$ the replacement of the solution in the measuring cell begins, and the concentration changes according to the relationship:[7]

$$c_{\mathrm{b}} = c_0 \exp(-t/\tau) \quad (2)$$

where c_0 is the protein or surfactant concentration in the bulk at $t = 0$, and $\tau = V/L$ is the time necessary for the replacement of the solution in the cell (in our experiments $\tau = 100$ s). The decrease of the bulk concentration c_{b} creates a diffusion flow from the bubble surface, which results in the decrease of adsorption according to the relation:

$$\left(\frac{\mathrm{d}\Gamma}{\mathrm{d}t}\right)_{\mathrm{D}} = -D\frac{c_{\mathrm{s}} - c_{\mathrm{b}}}{\delta} \quad (3)$$

where D is the diffusion coefficient, δ is the thickness of the hydrodynamic or diffusion boundary layer, and c_{s} is the subsurface concentration (assumed to be in equilibrium with the adsorption Γ). At $t = 0$ all concentrations are equal: $c_{\mathrm{s}} = c_{\mathrm{b}} = c_0$. It follows from eqs 2 and 3 that:

$$\left(\frac{\mathrm{d}\Gamma}{\mathrm{d}t}\right)_{\mathrm{D}} = -D\frac{c_{\mathrm{s}} - c_0 \exp(-t/\tau)}{\delta} \quad (4)$$

Using the Runge−Kutta method eq 4 can be solved. In this procedure the concentration dependencies of surface tension γ and adsorption Γ, calculated from the equilibrium isotherms for various theoretical models, were defined by polynomials of high order. The washing liquid enters into the lower part of the measurement cell. With increasing flow rate the unmixed boundary layer around the bubble decreases. The thickness of this so-called hydrodynamic boundary layer can be estimated from the formula $\delta = (\nu r/U)^{1/2}$, where r is the bubble radius, U is the velocity of the flow circumambient to the bubble, and ν is the kinematic viscosity of the liquid.[15] The U values for our cell were estimated by various methods to be in the range of 1 (no circulation) to 10 mm/s (with circulation). For a bubble radius of 2 mm we obtain δ values between 0.4 and 1.7 mm. Note, the circulation in the cell is generated by the tangential inflow of the washing liquid to the lower part of the cell, therefore a value of $\delta = 0.4$ mm is more reliable.

The theory of a barrier mechanism governing the desorption of surfactants and proteins was summarized in refs 9 and 14. The adsorption of protein in all possible states characterized by different molecular areas (see the equation of the adsorption isotherm (34) in ref 16) yields a Frumkin-type adsorption isotherm, including a factor accounting for such area variations. Thus, for surfactants and, approximately, for proteins if the area variations are relatively small the adsorption kinetics obeys the equation:[9,14]

$$\left(\frac{\mathrm{d}\Gamma}{\mathrm{d}t}\right)_{\mathrm{A}} = \beta c(0,t)(1-\theta) - \alpha\Gamma \exp(-2a\theta) \quad (5)$$

Here $\theta = \Gamma/\Gamma_\infty$ is the surface coverage, β and α are the adsorption and desorption rate constants, respectively, $\alpha = \beta/b\Gamma_\infty$, b is the adsorption equilibrium constant, a is the intermolecular attraction constant, t is the time, $c(0,t)$ is the subsurface concentration, and Γ_∞ is the limiting adsorption.

Adsorption and desorption involve the processes for overcoming an energy barrier so that the rate constants can generally be written in the form:[1,2,4,9]

$$\beta = \beta_0 \exp(-E_{\mathrm{a}}/RT) \quad (6)$$

$$\alpha = \alpha_0 \exp(-E_{\mathrm{d}}/RT) = \alpha_0 \exp[(-E_{\mathrm{a}} + E)/RT] \quad (7)$$

where E_{a}, E_{d}, and E are the adsorption activation energy, the desorption activation energy, and adsorption energy, respectively, and as preexponential factors the frequencies β_0 and α_0 correspond to the adsorption and desorption rates for the barrierless adsorption mechanism.

The desorption activation energy E_{d} (after Arrenius) and all its constituents in eq 7 can be assumed to be approximately

equal to the activation enthalpy ΔH (the experimental activation energy is by RT higher than the ΔH value, see ref 17) for $E_d \gg RT$. It should be noted that in a number of problems of molecular chemistry, such as recombinations of radicals[18] or reorganization of monolayers at the air/water interface,[19] the Gibbs free activation energy ΔG should be used instead of ΔH. This method is referred to as the variational transition state theory.[20] On the other hand, as the adsorption equilibrium constant b only slightly depends on the temperature, the contribution of the adsorption entropy to the adsorption enthalpy can be neglected (see below). The Gibbs' free energy of adsorption ΔG_0 can be expressed via the adsorption equilibrium constant b as:[13,21]

$$\Delta G_0 = -RT \ln(b\rho) \tag{8}$$

where ρ is the molar concentration of the solvent. For dilute aqueous solutions $\rho = 56$ mol/L (or 56×10^3 mol/m^3). For our experimental conditions it can be assumed, for the sake of simplicity, that $\theta \rightarrow 1$. Therefore, the first term on the right-hand side of eq 5 can be neglected and the maximum desorption rate is obtained:

$$(d\Gamma/dt)_A = -\alpha\Gamma_\infty \exp(-2a) \tag{9}$$

The first term in eq 5 is negligible also for arbitrary θ if the replacement of the solution by the solvent is sufficiently rapid. Then we can approximately assume $c(0,t) = 0$. Introducing α from eq 7 into eq 9, we obtain:

$$(d\Gamma/dt)_A = -\alpha_0\Gamma_\infty \exp(-2a) \exp(-E_d/RT) \tag{10}$$

Thus, from the temperature dependence of $(d\Gamma/dt)_A$ the activation energy of the desorption process can be calculated from eq 10, and this value could then be compared with the adsorption free energy calculated from eq 8.

Results and Discussion

Let us first consider the desorption kinetics for some surfactants. In ref 22 also the adsorption values for C_{13}DMPO were presented, obtained by a tensiometric method based on comparing the equilibrium surface tensions of solutions measured by a single drop and bubble, respectively. The dependencies of surface tension and adsorption of these surfactants on the concentration are well described by the Frumkin model:[13,21]

$$-\frac{\Pi\omega}{RT} = \ln(1-\theta) + a\theta^2 \tag{11}$$

$$bc = \frac{\theta}{1-\theta}\exp(-2a\theta) \tag{12}$$

Here $\omega = 1/\Gamma_\infty$ is the molar area, $\Pi = \gamma_0 - \gamma$ is the surface pressure, and γ_0 is the surface tension of solvent. The parameters involved in eqs 11 and 12 for the studied surfactants are the following:[13,22]

DeSNa: $\omega = 1.1 \times 10^5$ m^2/mol, $a = 0.8$, $b = 6.3 \times 10^{-2}$ m^3/mol

Triton X-100: $\omega = 3.87 \times 10^5$ m^2/mol, $a = -0.48$, $b = 3.74 \times 10^3$ m^3/mol

C_{13}DMPO: $\omega = 2.87 \times 10^5$ m^2/mol, $a = 0$, $b = 1.96 \times 10^3$ m^3/mol

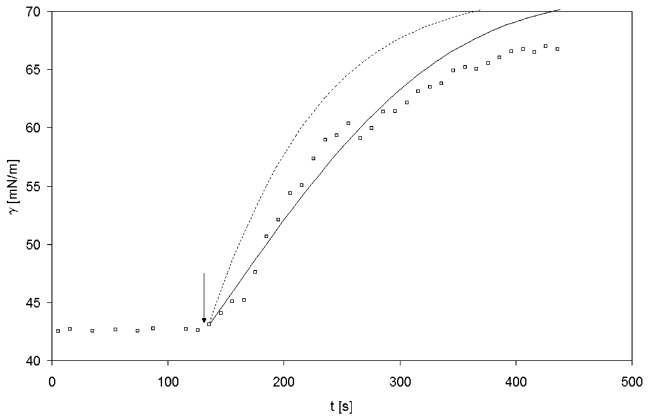

Figure 1. Dependence of surface tension of a DeSNa solution (concentration 0.02 mol/L) on time at 25 °C. The arrow indicates the initial time moment of washing the cell by the solvent. The theoretical curves were calculated from eq 4 for $\delta = 1.7$ (solid line) and 0.4 mm (dashed line).

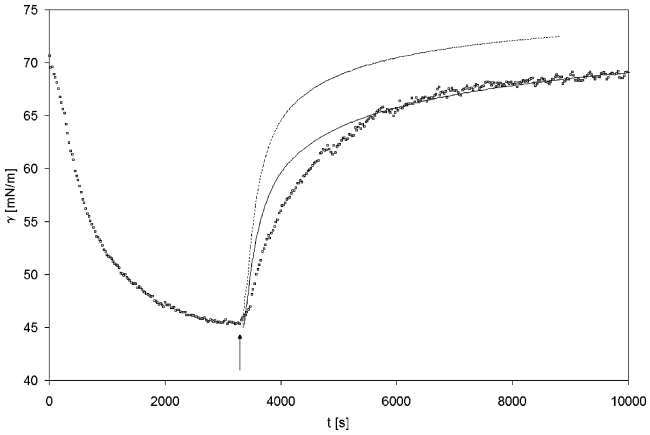

Figure 2. The same as in Figure 1 for C_{13}DMPO solution (concentration 2×10^{-5} mol/L).

Note that the surfactants in this study differ mainly in the b value: for the nonionic surfactants this value is 4 orders of magnitude higher than that for the ionic surfactant. To estimate possible differences resulting from the substitution of the free adsorption energy by the adsorption enthalpy in eq 7, Triton X-100 can be considered as an example. For Triton X-100 in the temperature range between 15 and 35 °C the value for b changes from 4.16×10^3 to 3.27×10^3 m^3/mol.[13] The ΔG_0 value calculated from eq 8 at 25 °C is −47.4 kJ/mol. The adsorption entropy calculated from the relation $\Delta S_0 = -(\partial \Delta G_0/\partial T)^1$ in this temperature range is $\Delta S_0 = -12.5$ J/(mol·K); therefore, $T\Delta S_0 = -3.7$ kJ/mol, and thus the difference between the ΔG_0 and $\Delta H_0 = \Delta G_0 + T\Delta S_0$ is less than 10%. The dependencies of dynamic surface tension for the DeSNa, C_{13}DMPO, and Triton X-100 solutions are presented in Figures 1−3, respectively. In all the experiments, the measuring cell was first filled by the surfactant solution (the capillary tip was initially filled by pure water to prevent the solution from rising into it), and a bubble of volume 25−30 mm^3 was formed. After the equilibrium was established (as shown by arrows) the process of replacement of the solution by pure water was started. It is seen that for all surfactants the adsorption process is reversible, because immediately after washing of the cell by the solvent was started, the surface tension increased. Figures 1−3 also show the theoretical dependencies of the dynamic surface tension during desorption, calculated from eqs 4, 10, and 11 of the diffusion model with parameters

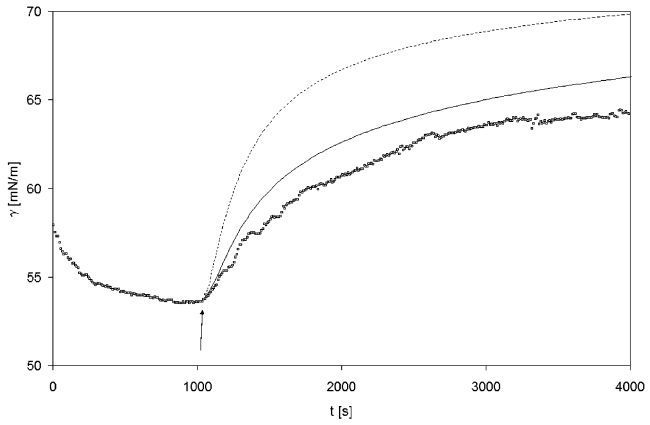

Figure 3. The same as in Figure 1 for Triton X-100 (concentration of 10^{-5} mol/L).

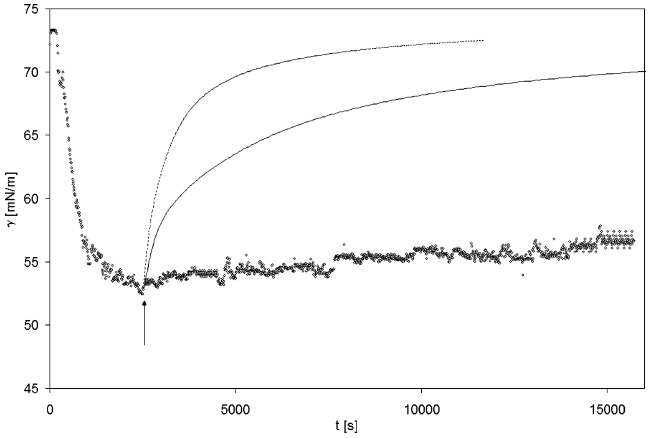

Figure 4. The same as in Figure 1 for a BLG solution (concentration 2×10^{-6} mol/L).

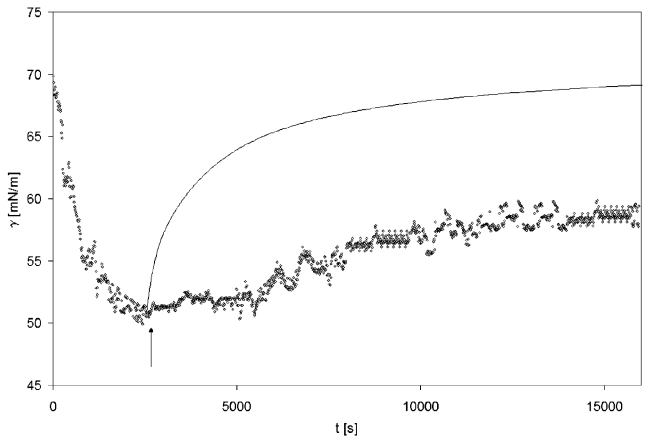

Figure 5. The same as in Figure 4 at 40 °C. The theoretical curve was calculated for $\delta = 1.7$ mm.

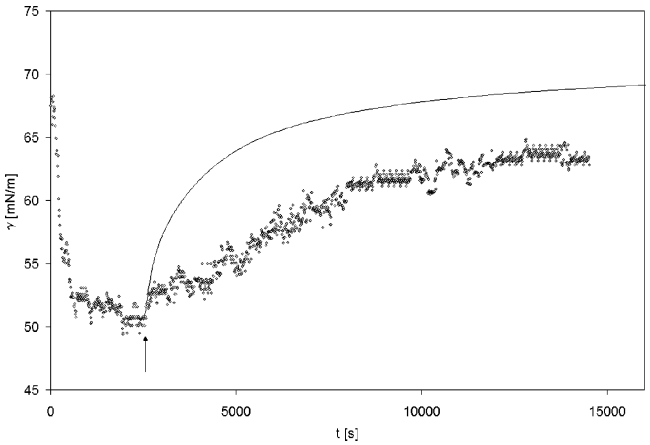

Figure 6. The same as in Figure 4 at 50 °C. The theoretical curve was calculated for $\delta = 1.7$ mm.

given above. The diffusion coefficient was taken equal to 3×10^{-10} m^2/s for DeSNa and 4×10^{-10} m^2/s for Triton X-100 and C_{13}DMPO, according to the actual D values for these surfactants.[11,13,21,22] For each experimental curve, two theoretical dependencies were calculated with values for δ in eq 4 equal to 0.4 (dotted line) or 1.7 mm (solid line). It is seen that the DeSNa desorption (Figure 1) is purely diffusion controlled, and the variation of δ only slightly affects the agreement between experiment and theory. Therefore, for DeSNa the limiting desorption rates obey the relation $(d\Gamma/dt)_D \ll (d\Gamma/dt)_A$. For C_{13}DMPO (Figure 2), and even more for Triton X-100 (Figure 3), the theoretical values, especially those calculated for the more realistic value $\delta = 0.4$ mm, are somewhat higher than the experimental data. This fact shows that the desorption of surfactants which possess high activity, like C_{13}DMPO and Triton X-100, is possibly governed by a mixed mechanism, but the absolute values of limiting rates obey the relation $(d\Gamma/dt)_D < (d\Gamma/dt)_A$. It can be supposed that this difference between these surfactants is due to the fact that their adsorption equilibrium constants b are very different, and, therefore, the free energy of adsorption for C_{13}DMPO and Triton X-100 is essentially higher, cf. eq 8. This, in turn, according to eq 7 can result in a significant decrease of the desorption rate coefficient α.

Now the results obtained for BLG solutions will be discussed. Figure 4 illustrates the BLG adsorption and desorption kinetics from a solution of concentration 2×10^{-6} mol/L. Similar results were obtained also for other BLG concentrations. In these experiments the cell was first filled by the buffer solution, then the buffer solution was replaced by the BLG solution, and then, after aging for 2500 s (as shown by arrow), the continuous replacement by a buffer solution was performed (buffer → BLG → buffer experiment). It is seen that the desorption process for BLG (in contrast to the adsorption process) is very slow. From the comparison with the diffusion model, eq 4 (using a diffusion coefficient of 10^{-10} m^2/s according to refs 23 and 24), it is clearly seen that for BLG the barrier mechanism of desorption is valid, i.e., the condition $(d\Gamma/dt)_A \ll (d\Gamma/dt)_D$ is satisfied. For the calculations according to eq 4 the equations of state of surface layer and adsorption isotherm derived in ref 16 with the parameters given in ref 25 were used. In particular, the b value for BLG is 5.27×10^4 m^3/mol, which is 15−25 times higher than that for the C_{13}DMPO and Triton X-100. It can be supposed that the higher adsorption equilibrium constant for BLG and, therefore, the higher free energy of adsorption lead to the slower kinetics of desorption of the protein.

If the activation energy of the desorption process is high, then it follows from eq 7 that the increase of temperature should increase the desorption rate constant α, and, therefore, the desorption rate. Figures 5 and 6 illustrate the results obtained for the same BLG concentration 2×10^{-6} mol/L at 40 and 50 °C. With increasing temperature, the BLG desorption rate becomes significantly higher. Nevertheless, from a comparison with the results calculated from the diffusion model, eq 4 (in the figures only one curve is shown, which corresponds to $D = 2 \times 10^{-10}$ m^2/s and $\delta = 1.7$ mm, most favorable with regard to the diffusion mechanism), it is seen that at these temperatures the inequality $(d\Gamma/dt)_A \ll (d\Gamma/dt)_D$ is still valid. It follows from Figures 4−6 that the equilibrium (at the initial time moment

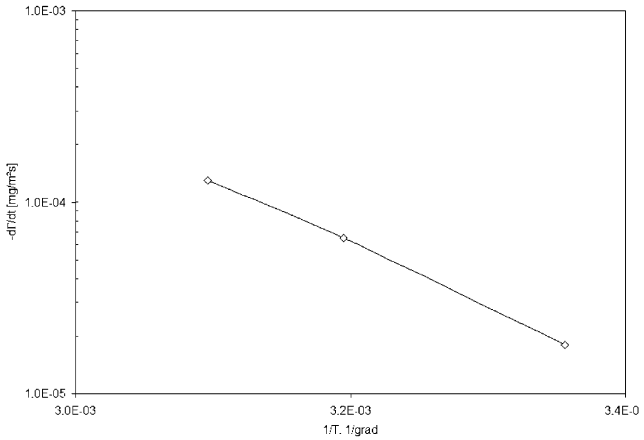

Figure 7. Dependence of BLG desorption rate on inverse temperature.

when washing of the cell by the solvent is started) surface pressure of the BLG solution is virtually independent of the temperature, and is approximately equal to 20 mN/m in the whole temperature range studied here. This fact indicates that the adsorption equilibrium constant for BLG only weakly depends on the temperature, and therefore one can substitute the adsorption energy by ΔG_0 in eq 7.

Figure 7 illustrates the dependence of $d\Gamma/dt$ on the inverse temperature, calculated from the initial sections of desorption curves shown in Figures 4−6 (using Γ vs Π dependence[25]). Assuming that the temperature dependence of the constants α_0 and Γ_∞ in eq 10 is weak, from eq 10 we obtain for the two compared temperatures T_1 and T_2 ($T_2 > T_1$):

$$\ln\left[\frac{(d\Gamma/dt)_{A2}}{(d\Gamma/dt)_{A1}}\right] = -\frac{E_d}{R}\left(\frac{1}{T_2} - \frac{1}{T_1}\right) \qquad (13)$$

Using the values of $(d\Gamma/dt)_A$ shown in Figure 7 we obtain from eq 13 the average value of the desorption activation energy for BLG in the studied temperature range as 64 kJ/mol.

From the BLG adsorption equilibrium constant $b = 5.27 \times 10^4$ m^3/mol eq 8 yields $\Delta G_0 = -55$ kJ/mol. According to ref 26, the activation energy of adsorption kinetics for globular proteins is $(2 \div 20)RT$, which agrees with our estimations $E_a = E_d + \Delta G_0 = 9$ kJ/mol, that is $E_a = 3.6RT$. Hence the experimental values of ΔG_0 and E_d are equal within the limits of experimental and calculation errors. In particular, the errors can be caused by neglecting the temperature dependence of the factor $\alpha_0\Gamma_\infty \exp(-2a)$ in eq 10, in which the values of a and Γ_∞ become lower, while α_0 becomes higher with increasing temperature. Therefore, as ΔG_0 and E_d are approximately equal to each other, the BLG adsorption mechanism is almost barrierless, in contrast to the barrier mechanism that was shown above to govern the desorption mechanism of this protein.

The lower desorption rate of the protein (in comparison to its adsorption rate) confirms one interesting phenomenon found experimentally for Bovine Plasma Albumin by Lucassen and Giles in 1971.[27] They demonstrated that the kinetics of protein adsorption from solution was accelerated by subjecting the surface to low-amplitude periodic expansion/compression deformations. This effect was attributed to the desorption in the compression stage being slower than the adsorption during the expansion part of each cycle. This leads to an increase in adsorption onto periodically deformed surfaces, which results in a faster or stronger decrease in surface tension. Figure 8 shows the results of similar experiments with nondeformed and deformed drop surfaces (oscillation frequency 0.017 Hz, magnitude ±7%, oscillation cycle duration 300 s, pause 300 s) for BLG solution with a concentration 10^{-6} mol/L. For the harmonically deformed drop surface, the surface tension is indeed lower than that for the nondeformed drop. Also, during the pauses between the oscillations, the surface tension clearly increases.

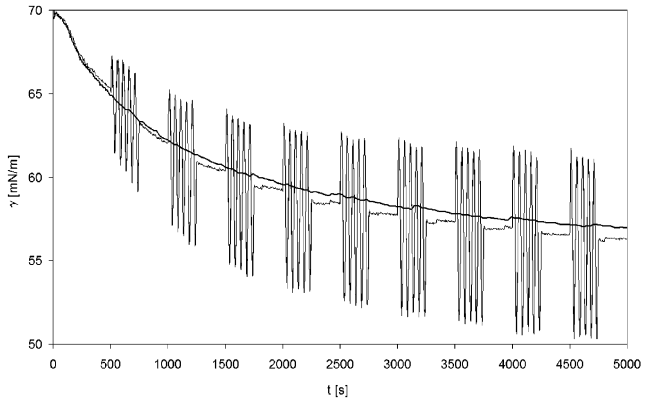

Figure 8. Dependence of surface tension of a BLG solution (concentration 10^{-6} mol/L) on time at 25 °C measured by the drop shape method. Thick curve: experiment without oscillations. Thin curve: experiment with the harmonic oscillations imposed on the drop surface.

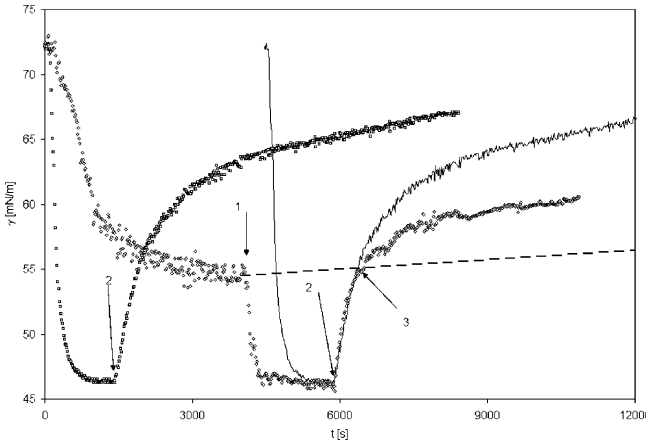

Figure 9. Dependence of surface tension of a Triton X-100 solution (◇, concentration 2×10^{-5} mol/L) and of a BLG solution (□, concentration 2×10^{-6} mol/L) on time at 25 °C. Arrow 1 indicates the initial time moment of washing out BLG from the cell by a Triton X-100 solution (2×10^{-5} mol/L); arrow 2 indicates the initial time moment of washing the cell by the solvent (buffer). The dotted line corresponds to the smoothed results shown in Figure 4 from the time moment when the washing of the cell by the buffer solution was started; the thin line reproduces the results (◇) with a time lag of 4450 s (to synchronize the starting moments of cell washing by the buffer solution in the two experiments).

Figure 9 shows the dynamic surface tension of a BLG solution (2×10^{-6} mol/L) starting from the value of the buffer. After 4000 s (as shown by arrow 1) the bulk phase is replaced by a $2\cdot \times 10^{-5}$ mol/L Triton X-100 solution (with buffer). After the equilibrium was attained (ca. 6000 s) the Triton X-100 solution was replaced by the pure buffer solution (arrow 2). For comparison, the dynamic surface tension for pure Triton X-100 at the same concentration is also shown in Figure 9. The same results are shown for clarity (by solid line) in Figure 9 with a suitable time lag to superimpose the starting moments of the replacement of the Triton X-100 solution by the buffer solution in the two experiments. Also in Figure 9 the results shown in Figure 4 for the replacement of the BLG solution by the solvent are reproduced as a dotted line.

Note that at the point marked by arrow 3 in Figure 9 (which is the point where the curves of the three experiments meet: buffer → BLG → buffer, buffer → BLG → Triton → buffer, and buffer → Triton → buffer) the rate of surface tension increase during the washing by the solvent in the buffer → BLG → Triton → buffer and buffer → Triton → buffer experiments is the same. Moreover, the rate of surface tension decrease during the Triton X-100 adsorption at the surface covered by BLG is equal to that obtained for Triton X-100 adsorption on a fresh surface, and the equilibrium surface tension value in these two experiments is almost identical, 46 mN/m, in agreement with ref 13. This fact indicates the preferential adsorption of Triton X-100 and BLG is replaced from the surface layer. The mechanism of this phenomenon is not very clear. It is possible that, in contrast to the desorption of BLG into the solvent, the protein molecule can desorb gradually, which requires lower activation energy. Another explanation of this phenomenon was proposed in refs 28 and 29, assuming that the protein is displaced by the surfactant in a way that it first forms 3-dimensional domains which then are displaced from the interface. Later this process was confirmed by Brewster angle microscopy (BAM) showing directly 3D structures at the water−air interface.[30,31]

Above the intersection point marked by arrow 3 the desorption kinetics curves for the three experiments become quite different: the most pronounced increase is observed for the buffer → Triton → buffer experiment, while for the buffer → BLG → Triton → buffer experiment this increase is lower, and it is still lower for the buffer → BLG → buffer experiment. These results indicate that the BLG is only partially washed out of the adsorption layer by the Triton X-100. It could be speculated that the three-dimensional domains of BLG existing at the surface are transformed again into a two-dimensional structure when the Triton X-100 is removed from the adsorption layer.

Conclusions

Models of diffusion, barrier, and mixed kinetics of desorption of surfactants and proteins from the adsorption layer at liquid/fluid interfaces are proposed. It is shown by experiments that the DeSNa desorption is governed by a pure diffusion mechanism, while desorption of more surface active surfactants such as C_{13}DMPO and Triton X-100 obeys a mixed mechanism. The BLG desorption kinetics, as shown by experiments, is determined by a barrier mechanism. From the analysis of the temperature dependence of the BLG desorption kinetics it is possible to calculate the activation energy of this process, which is quite close to the free energy of BLG adsorption. The theoretical model of desorption kinetics predicts that these two energetic parameters are approximately equal to each other if the adsorption activation energy is low. This can explain the fact that the higher the adsorption activity of a substance is, the lower is its desorption rate.

References and Notes

(1) Norde, W.; Haynes, C. A. In *Interfacial Phenomena and Bioproducts*; Brash, J. L., Wojciechowski, P. W., Eds.; Marcel Dekker: New York, 1999; p 123.

(2) Ramsden, J. J. In *Biopolymers at interfaces*; Malmsten, M., Ed.; Marcel Dekker: New York, 1999; p 321.

(3) Ramsden, J. J.; Roush, D. J.; Gill, D. S.; Kurrat, R. G.; Willson, R. C. *J. Am. Chem. Soc.* **1995**, *117*, 8511.

(4) Adamczyk, Z.; Szyk, L. *Langmuir* **2000**, *16*, 5730.

(5) Gonzalez, G.; MacRitchie, F. *J. Colloid Interface Sci.* **1970**, *32*, 55.

(6) MacRitchie, F. In *Proteins at Liquid Interfaces*; Studies of Interface Science, Vol. 7; Möbius, D., Miller, R., Eds.; Elsevier: Amsterdam, The Netherlands, 1998; p.149.

(7) Svitova, T. F.; Wetherbee, M. J.; Radke, C. J. *J. Colloid Interface Sci.* **2003**, *261*, 170.

(8) Wege, H. A.; Holgado-Terriza, J. A.; Neumann, A. W.; Cabrerizo-Vilchez, M. A. *Colloids Surf. A* **1999**, *156*, 509.

(9) Miller, R.; Grigoriev, D. O.; Krägel, J.; Makievski, A. V.; Maldonado-Valderrama, J.; Leser, M.; Michel, M.; Fainerman, V. B. *Food Hydrocolloids* **2005**, *19*, 479.

(10) Miller, R.; Olak, C.; Makievski, A. V. *SOFW* (*Engl.*) **2004**, 2−10.

(11) Czichocki, G.; Makievski, A. V.; Fainerman, V. B.; Miller, R. *Colloids Surf. A* **1997**, *122*, 189.

(12) Fainerman, V. B.; Makievski, A. V.; Vollhardt, D.; Siegel, S.; Miller, R. *J. Phys. Chem. B* **1999**, *103*, 330.

(13) Fainerman, V. B.; Miller, R.; Aksenenko, E. V.; Makievski, A. V. In *Surfactants−Chemistry, Interfacial Properties and Application*; Studies in Interface Science, Vol. 13; Fainerman, V. B., Möbius, D., Miller, R., Eds.; Elsevier: Amsterdam, The Netherlands, 2001; pp 189−286.

(14) Miller, R.; Joos, P.; Fainerman, V. B. *Adv. Colloid Interface Sci.* **1994**, *49*, 249.

(15) Levich, V. G. *Physicochemical hydrodynamics*; Prentice Hall: Englewood Cliffs, NJ, 1962.

(16) Fainerman, V. B.; Lucassen-Reynders, E. H.; Miller, R. *Adv. Colloid Interface Sci.* **2003**, *106*, 237.

(17) Glasstone, S.; Laidler, K. J.; Eyring, H. *The Theory of Rate Processes*; McGraw-Hill Book Co.: New York, 1941.

(18) Jensen, F. *Introduction to Computational Chemistry*; John Wiley & Sons: Chichester, UK, 1999.

(19) Vysotsky, Yu. B.; Bryantsev, V. S.; Fainerman, V. B.; Vollhardt, D.; Miller, R.; Aksenenko, E. V. *J. Phys. Chem. B* **2004**, *108*, 8330.

(20) Truhlar, D. G.; Gordon, M. S. *Science* **1990**, *249*, 491.

(21) Fainerman, V. B.; Miller, R.; Möhwald, H. *J. Phys. Chem. B* **2002**, *106*, 809.

(22) Fainerman, V. B.; Lylyk, S. V.; Makievski, A. V.; Miller, R. *J. Colloid Interface Sci.* **2004**, *275*, 305.

(23) Feijter, J. A de; Benjamins, J.; Veer, F. A. *Biopolymers* **1978**, *17*, 1760.

(24) Sober, H. A., Ed. *Handbook of Biochemistry*; Chemical Rubber Co.: Cleveland, OH, 1968.

(25) Fainerman, V. B.; Zholob, S. A.; Leser, M. E.; Michel, M.; Miller, R. *J. Phys. Chem. B* **2004**, *108*, 16780.

(26) Damodaran, S. *Curr. Opin. Colloid Interface Sci.* **2004**, *9*, 328.

(27) Lucassen, J. Private communication.

(28) Mackie, A. R.; Gunning, A. P.; Wilde, P. J.; Morris, V. J. *Langmuir* **2000**, *16*, 2242.

(29) Mackie, A. R.; Gunning, A. P.; Wilde, P. J.; Morris, V. J. *J. Colloid Interface Sci.* **1999**, *210*, 157.

(30) Mackie, A. R.; Gunning, A. P.; Ridout, M. J.; Wilde, P. J.; Patino, J. R. *Biomacromolecules* **2001**, *2*, 1001.

(31) Patino, J. M. R.; Nino, M. R. R.; Sanchez, C. C.; Fernandez, M. C. *Langmuir* **2001**, *17*, 7545.